Tree Physiology 00, 1–12
https://doi.org/10.1093/treephys/tpad015

Methods paper

An incubation method to determine the age of available nonstructural carbon in woody plant tissues

Drew M.P. Peltier[1,3,4], Jim Lemoine[1], Chris Ebert[1], Xiaomei Xu[2], Kiona Ogle[1,3], Andrew D. Richardson[1,3] and Mariah S. Carbone[1]

[1]Center for Ecosystem Science and Society, Northern Arizona University, Flagstaff, AZ 86011, USA; [2]Department of Earth System Science, University of California, Irvine, CA 92617, USA; [3]School of Informatics, Computing, and Cyber Systems, Northern Arizona University, Flagstaff, AZ 86011, USA; [4]Corresponding author (dmp334@nau.edu)

Received August 21, 2022; accepted February 3, 2023; handling Editor Simon Landhäusser

Radiocarbon ($\Delta^{14}C$) measurements of nonstructural carbon enable inference on the age and turnover time of stored photosynthate (e.g., sugars, starch), of which the largest pool in trees resides in the main bole. Because of potential issues with extraction-based methods, we introduce an incubation method to capture the $\Delta^{14}C$ of nonstructural carbon via respired CO_2. In this study, we compared the $\Delta^{14}C$ obtained from these incubations with $\Delta^{14}C$ from a well-established extraction method, using increment cores from a mature trembling aspen (*Populus tremuloides Michx*). To understand any potential $\Delta^{14}C$ disagreement, the yields from both methods were also benchmarked against the phenol-sulfuric acid concentration assay. We found incubations captured less than 100% of measured sugar and starch carbon, with recovery ranging from ~3% in heartwood to 85% in shallow sapwood. However, extractions universally over-yielded (mean 273 ± 101% expected sugar carbon; as high as 480%), where sugars represented less than half of extracted soluble carbon, indicating very poor specificity. Although the separation of soluble and insoluble nonstructural carbon is ostensibly a strength of extraction-based methods, there was also evidence of poor separation of these two fractions in extractions. The $\Delta^{14}C$ of respired CO_2 and $\Delta^{14}C$ from extractions were similar in the sapwood, whereas extractions resulted in comparatively higher $\Delta^{14}C$ (older carbon) in heartwood and bark. Because yield and $\Delta^{14}C$ discrepancies were largest in old tissues, incubations may better capture the $\Delta^{14}C$ of nonstructural carbon that is actually metabolically available. That is, we suggest extractions include metabolically irrelevant carbon from dead tissues or cells, as well as carbon that is neither sugar nor starch. In contrast, nonstructural carbon captured by extractions must be respired to be measured. We thus suggest incubations of live tissues are a potentially viable, inexpensive and versatile method to study the $\Delta^{14}C$ of metabolically relevant (available) nonstructural carbon.

Keywords: allocation, bomb-spike, heartwood, NSC, *Populus tremuloides*, radiocarbon.

Introduction

Woody plants store photosynthate as nonstructural carbon, serving (among other roles, e.g., Wang and Stutte 1992) as metabolic substrate in the absence of favorable climate conditions for new photosynthesis (Kozlowski, 1992). Although lipids, sugar alcohols, amino acids and other compounds play roles in storage (Hoch et al. 2003, Dietze et al. 2014), sugars and starch are often considered the major components of this pool and are most commonly measured (Quentin et al. 2015, Landhäusser et al. 2018). In long-lived trees, total nonstructural carbon can be large relative to tree biomass (Hoch et al. 2003), and include carbon fixed from the atmosphere decades prior (Richardson et al. 2013). Some of this old carbon remains labile, or 'available' for remobilization and respiration, notably during periods of severe stress or disturbance (Vargas et al. 2009, Carbone et al. 2013, Muhr et al. 2018). The study of nonstructural carbon pool sizes and turnover times thus can improve understanding of tree resilience to stress and

disturbance. For example, reliance on old nonstructural carbon is an appealing explanation for observed 'memory' of tree growth (Rocha et al. 2006, Carbone et al. 2013, Peltier et al. 2018).

Although nonstructural carbon turnover times can be studied through intensive isotope labelling studies (Matamala et al. 2003, Carbone et al. 2007, Carbone and Trumbore 2007, Plain et al. 2009, Epron et al. 2012) background abundance radiocarbon (^{14}C) measurements can provide estimates (1–3 year resolution; Hua and Barbetti 2004) of the mean age of nonstructural carbon (Richardson et al. 2013). This is made possible by reference to the bomb-spike of ^{14}C (Levin and Kromer 2004), a byproduct of atmospheric thermonuclear weapons testing terminating with the Partial Test Ban Treaty in 1963. These historical events approximately doubled the concentration of ^{14}C in the atmosphere, since a combination of biogeochemical processes and anthropogenic carbon emissions have led to steady declines in the atmospheric ^{14}C concentration, creating a unique, high-resolution tracer (Keeling, 1979, Schuur et al. 2016). Thus, it is possible to quantify the time elapsed since carbon was fixed from the atmosphere in organic matter (Cain and Suess 1976, Vargas et al. 2009, Trumbore et al. 2015, Muhr et al. 2016). Previous work found the mean age of nonstructural carbon (e.g., sugars) in tree rings increases with depth into the main bole and is younger than structural carbon (e.g., cellulose) (Richardson et al. 2015, Trumbore et al. 2015). However, the small number of existing studies have been necessarily limited in sample size and spatial extent. Broader application of $\Delta^{14}C$ measurements of nonstructural carbon is essential to understand the size, turnover time and ultimately the relevance of growth and metabolism of old reserves across forested ecosystems under ongoing climate change and disturbance.

An extraction method developed to study the $\Delta^{14}C$ of nonstructural carbon (Czimczik et al. 2014) has been used in a number of influential studies (Carbone et al. 2013, Richardson et al. 2013, 2015, Trumbore et al. 2015) but exploratory work with *Populus tremuloides* Michx. found extractions appeared to overestimate the concentrations of available nonstructural carbohydrates (NSC, sugars and starch) and suffer from issues of specificity, particularly in the bark. Similar issues have been occasionally noted in the literature (e.g., Trumbore et al. 2015). For example, nonstructural carbon available for use by the tree could be overestimated when extracting from older tissues containing some dead cells like heartwood and/or bark that may still contain nonstructural carbon (Gartner et al. 2000). Past work also suggests available methods of isolation of 'sugar' and 'starch' fractions (defined in Materials and methods) for carbon isotope measurements are not highly specific, where only ~ 50% of extracted material may be sugars (Richter et al. 2009, Trumbore et al. 2015), with the remaining material being unknown. For example, acid hydrolysis of starch can solubilize other water insoluble carbon (e.g., hemicellulose) (Richter et al. 2009). Alternative enzymatic methods for isolation of specific compounds have also been shown to produce variable carbon isotopic values (Richter et al. 2009). Although methods exist to purify sugar extracts for stable isotope analysis (Rinne et al. 2012, Lehmann et al. 2017), $\Delta^{14}C$ from similarly purified extracts was nonsensical (e.g., −100%), perhaps due to greater sensitivity of $\Delta^{14}C$ to contamination. Regardless of whether extractions isolate nonstructural carbon by solubility (Czimczik et al. 2014), or identify nonstructural carbon by color formation (Landhäusser et al. 2018) or other detection methods (Raessler et al. 2010), measurable nonstructural carbon may be an overestimate of available nonstructural carbon for metabolism. Furthermore, osmoregulation is a key function of soluble sugars and sugar alcohols where some minimum concentration of these osmolytes is required to maintain cell turgor (Wang and Stutte 1992) at any given time, and so this fraction of nonstructural carbon may not function as reserves, even if accurately measured.

To address these issues, we developed an alternative, incubation method for ^{14}C quantification of available nonstructural carbon in tree tissues. We compared a well-established method to extract nonstructural carbon for ^{14}C analysis (Czimczik et al. 2014) with a live-incubation method in a ~30-year-old trembling aspen (*P. tremuloides*) to ask the following questions: (Q1) How do extraction and incubation methods differ across tissues of varying age? Although similar incubations have been used before for different aims (e.g., Schuur and Trumbore 2006, Hilman et al. 2021), we present here a standardized protocol (Methods S1 available as Supplementary data at *Tree Physiology* Online) to study the size and age of the total available nonstructural carbon pool, which we validate against an established method. In short we seek to test if incubations capture the size and age of the available nonstructural carbon pool. We define 'available' nonstructural carbon to include the nonstructural carbon that could be remobilized for metabolic needs (excluding sugars serving to regulate osmotic potential, osmotica). For replicate samples, we thus compared carbon mass (extracted vs respired) and $\Delta^{14}C$ (extracted vs respired) for four key bole tissues (bark, shallow sapwood, deep sapwood and heartwood). Carbon yields from both incubation and extraction methods were further benchmarked against expected yields based on concentration measurements of sugar and starch (Landhäusser et al. 2018). In this way, we can explicitly distinguish between four non-identical carbon quantities: (i) the true amount of nonstructural carbon (not all of which is available); (ii) the carbon isolated from extractions; (iii) the carbon measured via concentration measurements targeted at sugars and starch; and (iv) the carbon respired from incubations.

We also asked: (Q2) Is the $\Delta^{14}C$ measured on respired carbon robust to incubation duration? The incubation method relies on CO_2 production from cellular respiration of nonstructural carbon. Because total tree nonstructural carbon is not a

well-mixed pool (Herrera-Ramírez et al. 2020), where older carbon is found in older tissues (Richardson et al. 2015), girdled trees and coarse roots have been shown to respire progressively older carbon with time (Muhr et al. 2018, Hilman et al. 2021). It is sometimes then assumed that this 'reverse chronological mobilization' or 'first-in last-out' (Lacointe et al. 1993, Carbone et al. 2013) process also occurs at the tissue or even cellular level, for example, following the so-called 'onion model' of starch granule formation (Badenhuizen and Dutton 1956, Pilling and Smith 2003). Because incubations cannot capture 100% of nonstructural carbon, strong reverse chronological mobilization would imply $\Delta^{14}C$ from incubations would not be representative of the total reserve pool (as the oldest carbon would be left unrespired). To directly test this assumption, respiration samples were also collected at intermediate time increments of 24, 72 and 120 h after sampling to demonstrate respired $\Delta^{14}C$ does not meaningfully change across time, at least in this species.

Materials and methods

We harvested a vigorous, canopy-dominant, ~20 m high, 19-cm diameter trembling aspen (*P. tremuloides*) near Flagstaff, Arizona (35.387, −111.775) during a single morning in September of 2020 (Figures S1 and S2 available as Supplementary data at *Tree Physiology* Online). This site (2460 m a.s.l.) is in the middle of this species' elevational range in Arizona (~1980–3050 m). *Populus tremuloides Michx.* has wide, easily identifiable tree rings and high respiration rates, making it very suitable for the incubation method (described below). This species stores appreciable concentrations of lipids (Grimberg et al. 2018). However because the only existing radiocarbon extraction method does not explicitly target them (Czimczik et al. 2014, described below), and sugars and starch are the most commonly measured nonstructural carbon (Quentin et al. 2015, Landhäusser et al. 2018), we do not quantify lipids. However, we note that the incubation method (described below) likely captures lipids if they can be respired.

Prior to felling, four replicate cores (three for incubation time-series, one for extractions; Table 1) were collected with an unlubricated increment borer (12 mm, Haglöf, Sweden) from ~0.9 m height on the north side of the tree, in very close proximity to each other. Phloem sap may have been carried onto xylem tissues from the coring process, which may have introduced some error to subsequent measurements (see below). After incubations were initiated (below), the tree was felled with a reciprocating saw (oil-free blade), and after transport on ice, 3–5 cm cross sections were collected with an oil-free miter saw. These sections were frozen at −20 °C within 5 h of tree felling, and subsequently freeze-dried (FreeZone 2.5, Labconco, Kansas City, MO, USA and Hybrid Vacuum Pump, Vaccubrand, Wertheim, Germany). Tree ring widths were measured along two radii (north and south) on a cross-section from a 1.37-m height. Pith date at this height was 1991, making the tree at least 29 years old at harvest. A full methodological workflow is depicted in Figure S2 available as Supplementary data at *Tree Physiology* Online.

Incubations of live wood to obtain respired CO_2

The incubation method (Table 1) assumes the ^{14}C of nonstructural carbon used as substrate for respiration is representative of the pool of all available NSC within live-tissue sections, and we also directly test this assumption with Q2 (below). To address Q1, we compared results (yield, $\Delta^{14}C$) from incubations with those of extractions (described below) on replicate tree cores. Thus, three of four replicate increment cores were used for incubations in the field. These three cores were mounted on a vice, surfaced with a razor blade to visualize ring boundaries, and separated into three sections: the outermost six rings (rings 1–6, hereafter, 'shallow sapwood'), the next six rings (rings 7–12, hereafter 'deep sapwood') and an additional six rings (rings 13–18, hereafter 'heartwood'). Ring 13 was transitional between sapwood and heartwood; thus, this last section (rings 13–18) represented largely heartwood. *Populus tremuloides Michx.* retains a green photosynthetic periderm under the exterior of the bark (Pearson and Lawrence 1958), and much of the bark cross-section remains hydrated, exhibiting high respiration rates and sugar and starch concentrations (Wiley et al. 2019). Thus, the entire bark tissue, including the phloem, was also separated from the increment core and incubated (hereafter, 'bark'). The three xylem sections and bark (4 tissues × 3 replicates) were sealed in 256-ml mason jars with custom two-port lids (Luer-lock fittings with valves), and the jars were immediately purged for 60 s each with CO_2-free air containing oxygen (Ultrazero air, Airgas). Using this flushing method, we estimated remaining atmospheric CO_2 constitutes ~1% of ultimate headspace CO_2 (described in Methods S1 available as Supplementary data at *Tree Physiology* Online). In all cases, time from core collection to initiation of incubation was less than 30 min (<0.5% of total respired carbon); thus, these cores were alive and actively respiring when incubations began.

To address Q2, we quantified a time-series of total carbon respired (mass) and its mean age (see section Accelerator mass spectrometry and $\Delta^{14}C$). Jars ($n = 12$) were subsequently transported to a climate-controlled lab space and incubated in darkness at room temperature (Table 1) for either 24, 72 or 120 h. At 24 h, headspace air was collected into an evacuated, 1-l air-stabilizer can (Lab Commerce, San Jose, CA, USA). One replicate incubation each for all four tissues was then terminated by freezing ($n = 4$, rep 1). The remaining replicate incubation jars ($n = 8$, reps 2 and 3) were then resealed and re-purged, and those incubations were allowed to continue. Headspace air collection was repeated at 72 h, where only the third replicate of each tissue was again purged, resealed and allowed to continue ($n = 4$, rep 3). At 120 h, headspace air was similarly collected

Table 1. Overview of the incubation method, with reference to a more detailed procedure in Methods S1 (available as Supplementary data at Tree Physiology Online).

Step	Details	Procedure
Preparation	Avoid contamination, construct incubation jars	A, B
Field sampling	Collect increment core and sub-sample sapwood sections	C
Flushing	Scrub or flush atmospheric CO_2 from chamber headspace	D.1–D.3
Incubation	Incubate chambers for 120 h for CO_2 respiration	D.4
Concentration measurement	Assess concentration of respired CO_2 in the headspace	E
Headspace collection	Flush headspace into a stabilizer can	F
Purify CO_2	Remove nitrogen, water and other gases from gas sample	G
Make graphite	Convert CO_2 to graphite for AMS	H

($n = 4$, rep 3) and incubations were terminated (Figure S2 available as Supplementary data at *Tree Physiology* Online). Thus, samples were collected representing a time-series of respiration over 0–24, 24–72 and 72–120 hours. To calculate total mass of carbon respired (mg), headspace CO_2 concentrations at these intermediate time points were measured via 5-ml sub-samples on a LI6262 IRGA (Li-Cor, Lincoln, NE, USA) by comparison with a standard curve of gases with known concentrations (201, 380, 2070, 4000, 10,000 and 50,000 p.p.m.). Heartwood samples produced little CO_2, and respired carbon mass was measured directly on a vacuum line during ^{14}C preparation (see section Accelerator mass spectrometry and $\Delta^{14}C$). The third incubation tissue replicates (120-h incubation time) were also subsequently freeze-dried and ground for post-incubation sugar and starch concentration determination.

Extractions of dried wood to obtain nonstructural carbon

The fourth replicate core was flash-frozen on dry-ice in the field, freeze-dried, sectioned identically to incubation samples, and ground to 20 mesh on a Wiley mill (Thomas Scientific Wiley Mill, Swedesboro, NJ, USA). The relatively coarse grind used for this method is necessary to achieve proper separation of supernatant and solids at various steps, but particularly when isolating the insoluble fraction ('starch'). Subsequently, these samples were processed according to an established extraction method to obtain soluble and insoluble nonstructural carbon for $\Delta^{14}C$ (Czimczik et al. 2014). This method was developed to extract nonstructural carbon from vegetation samples while minimizing contamination via carbon-based solvents (ethanol, methanol) that can bias $\Delta^{14}C$ values. Contamination is particularly evident if solvent carbon is derived from fossil fuel sources (i.e., highly depleted, $\Delta^{14}C \ll 0$), but harder to detect when solvent carbon is modern. Two fractions are operationally defined in the protocol as 'sugars' (the nonstructural carbon soluble in water) and 'starch' (the nonstructural carbon obtained from subsequent acid hydrolysis; Richter et al. 2009, Czimczik et al. 2014). Thus, unlike the incubation method, $\Delta^{14}C$ can be quantified independently for both fractions.

To briefly summarize the method, ground samples are extracted in three rounds of boiling water, centrifuged, and the resulting solution is subsequently freeze-dried to obtain the 'sugars' (soluble nonstructural carbon) fraction. Subsequently, the remaining pellet is serially extracted (more than five rounds) with boiling 80% ethanol until the resulting solution is colorless to remove non-polar compounds (e.g., lipids), and then treated by acid hydrolysis with 20% HCl to solubilize remaining nonstructural carbon (i.e., starch). This solution is centrifuged, with care to exclude fine particles, and the insoluble fraction is precipitated with 100% ethanol (starch is insoluble in ethanol). The resulting solids are then serially re-dissolved in water and partially freeze-dried (three to five rounds) to remove trace amounts of ethanol, then completely freeze-dried.

Compared with typical sugar and starch concentration measurements (Landhäusser et al. 2018), large amounts of dry sample material (>500 mg) are sometimes required to obtain sufficient 'starch' carbon for a $\Delta^{14}C$ measurement (target 1-mg carbon, Czimczik et al. 2014), suggesting some starch may be extracted in the soluble fraction. But this also may impact extraction efficiency of the 'sugars' step. Thus, to understand the composition of soluble nonstructural carbon, we sent extracts to an analytical lab (Celignis, Castletroy, Ireland) to be analyzed via High-Performance Anion-Exchange chromatography with Pulsed Amperometric Detection (HPAE-PAD). Finally, to assess the dependence of the ^{14}C extraction carbon yield on initial dry mass, additional replicate extractions were similarly carried out (soluble fraction only) for aspen twigs, bulk sapwood and bark. We focus this last analysis on soluble nonstructural carbon ('sugars') as insoluble nonstructural carbon ('starch') constitutes a small fraction of total nonstructural carbon (see Results) and did not impact results for a subset of samples.

We then compared each of (i) carbon content (mg) obtained from this extraction method and (ii) incubation carbon masses (above) with (iii) an 'expected' nonstructural carbon mass from sugar and starch concentration assays (below). This 'expected' carbon mass was calculated by applying sugar and starch concentrations to initial sample dry masses from either (i) ^{14}C extractions or (ii) incubations.

Sugar and starch concentrations

Rings were individually separated with a narrow chisel from three freeze-dried cross-sections taken between 1.3 and 1.4 m height and ground to a fine powder (Retsch MM200 ball

mill, Haan, Germany). To be consistent with collected cores, north side wood was included in these samples (270°—90° orientation) and the entire north side wood from the three cross-sections was homogenized for each ring. Soluble sugar and starch concentrations were measured for individual rings, for rings 1–18 and the bark using the standard and widely used phenol-sulfuric acid method as in (Furze et al. 2019), the uncertainties of which and protocols for minimizing uncertainty are given in Landhäusser et al. (2018). Briefly, ~40 mg of sample is extracted in three rounds of boiling ethanol (5 ml each). Absorbance is read at 490 nm using spectrophotometer (GENESYS 10S UV-Vis, Thermo-Fisher Scientific, USA) and calibrated against a glucose-fructose-galactose standard curve. Starch in the pellet is subsequently converted to glucose using alpha-amylase followed by amyloglucosidase (Sigma-Aldrich, USA) at 50 °C, and absorbance is similarly read at 525 nm and compared with a glucose standard curve. We simultaneously measure an in-house standard (*Quercus rubra* L. wood) with each run, the running coefficient of variation (CV) of this standard is 0.10 for sugar and 0.11 for starch.

Concentrations were determined from cross sections, and were aggregated by ring width (weighted averaging) to generate total NSC concentrations for each tissue (shallow sapwood, deep sapwood, heartwood). Because replicate cores taken from slightly different (but adjacent) locations were used for $\Delta^{14}C$ measurements, variability in sugar and starch concentrations from both measurement error and spatial variation is averaged over in this approach. Samples used in the incubation method were also analyzed for concentrations to determine how much sugar and starch remained after incubation.

Accelerator mass spectrometry and $\Delta^{14}C$

Freeze-dried extracts were combusted to CO_2 in the presence of cupric oxide under vacuum in quartz tubes (Boutton et al. 1983). CO_2 from incubations and combusted extracts was then purified on a vacuum line and subsequently converted into graphite (Lowe, 1984, Vogel et al. 1984). The ^{14}C content of graphite was analyzed on a MICADAS (IonPlus, Switzerland; Synal et al. 2007) at the Arizona Climate and Ecosystems (ACE) isotope laboratory at Northern Arizona University (Flagstaff, AZ, USA). Values are corrected for mass-dependent fractionation by normalizing to common $\delta^{13}C$ (−25%) under the assumption that ^{14}C fractionates twice as much as ^{13}C (Stuiver and Polach 1977). Data are reported as decay corrected $\Delta^{14}C$ (%) according to (Reimer et al. 2004) and Fraction Modern ($F^{14}C$) values, as the sample ratio of $^{14}C/^{12}C$ divided by that of a standard, are reported in Table S1 available as Supplementary data at *Tree Physiology* Online. Modern standards (Oxalic acid II) run at both WM Keck Carbon Cycle AMS Facility (UC-Irvine, Irvine, CA, USA) and NAU have a standard deviation of ±2%. We estimate sample ages (years since fixation) from $\Delta^{14}C$ by comparing with an annual atmospheric record of the bomb curve for the northern hemisphere (zone 2) boreal summer (Hua et al. 2021). Importantly, this only provides information about the mean age of a given pool of carbon (e.g., shallow sapwood soluble nonstructural carbon).

Results

Sugar and starch concentrations

The tree had narrow rings in 1996, 2006 and 2018, coincident with dry years in northern Arizona (Figure 1a), as the harvested tree was representative of a typical *P. tremuloides* in the southwestern USA. Concentrations of sugars and starch were highest in the most recently formed ring (2.45 and 0.36%, respectively). Sugar and starch concentrations dropped to ~0 at the sapwood–heartwood boundary (Figure 1b and c). Starch concentrations remained ~0 in heartwood tree rings (Figure 1c), whereas measured sugar concentrations increased with depth into the heartwood (Figure 1b). High sugar concentrations measured in the heartwood may be an artifact of incomplete removal of interference from heartwood extractives (phenolics) by the 'blank' during the phenol-sulfuric acid method (Landhäusser et al. 2018). They could also reflect sugars that are simply locked away in heartwood and unusable.

Incubation carbon yield

Shallow sapwood and deep sapwood respired CO_2 equivalent to 85 and 51%, respectively, of expected nonstructural carbon (based on sugar + starch concentrations) (Figure 2a). In contrast, heartwood respired almost none (~3%), whereas bark respired only 22% (Figure 2a). We obtained similar incubation carbon mass yields from sugar and starch concentration measurements conducted post-incubation, except in heartwood. According to these 'post-incubation NSC concentrations', incubations exhausted 82 and 58% of sugar and starch in shallow sapwood and deep sapwood, respectively, 32% in bark and 42% in heartwood. Incubations indicate starch was almost completely exhausted before sugar was depleted, despite lower initial concentrations of this fraction: 93 and 90% of starch were exhausted in the shallow and deep sapwood, respectively, compared with 44% and 26% of sugars for the same tissues. In comparison, 65% and 41% of starch were exhausted in bark and heartwood, respectively, compared with 22% and 42% of sugars for the same tissues. Because of larger initial sugar concentrations, this still indicates a larger mass of sugar was respired than of starch. We again note that the discrepancy in heartwood between respired CO_2 (3% nonstructural carbon) and remaining sugar and starch C (42 and 41%, respectively) is likely due to interfering compounds (phenolics), where sugar concentration measurements in heartwood may not be accurate, exacerbated by the small amount of measurable nonstructural carbon (pre-incubation heartwood starch concentrations were essentially zero; Figure 1c).

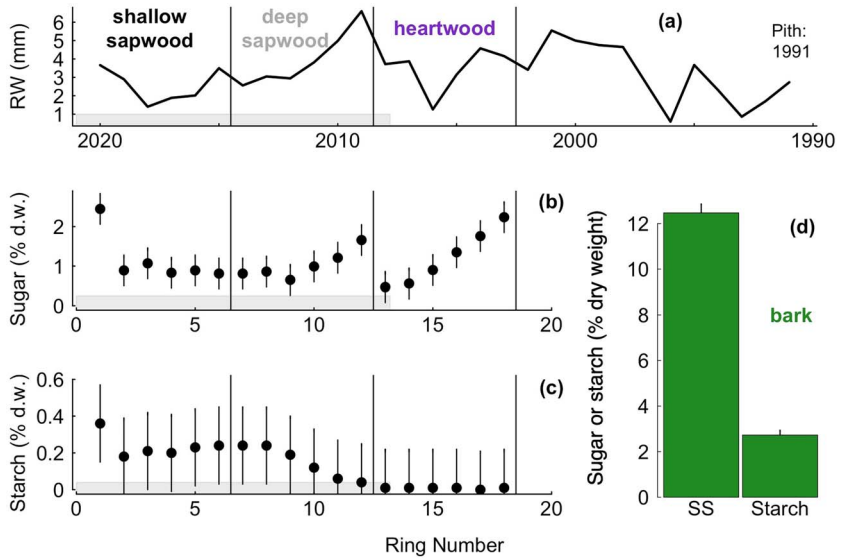

Figure 1. Ring widths (a), ring-wise soluble sugar (b) and starch (c) concentrations, and living bark ('bark') sugar and starch concentrations (d) for the *P. tremuloides* tree harvested in September 2020 near Flagstaff, Arizona. Sugar and starch concentrations are reported as % dry weight ('d.w.'). Horizontal gray shading along the *x*-axis in (a–c) denotes the extent of active sapwood rings. This tree was ~ 30 years old with a pith date of 1991. Tree ring depths are denoted as shallow sapwood, deep sapwood and heartwood, with boundaries marked by vertical black lines. Vertical lines in (b–d) denote standard deviation from repeat measurement of an in-house wood standard during sample runs.

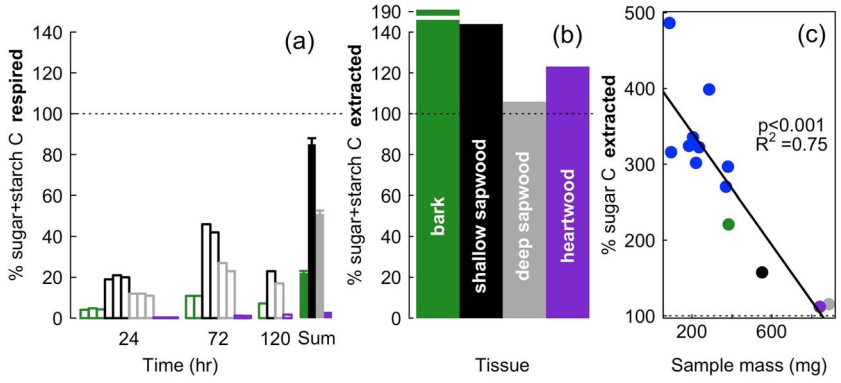

Figure 2. (a) Incubation-based ^{14}C method yields similar amount of carbon to that expected from sugar and starch concentration measurements in the shallow sapwood, whereas (b) extraction-based methods generally over-yield across all tissues, (c) contingent on sample mass. In (a), for bark (green), shallow sapwood (black), deep sapwood (gray) and heartwood (purple), unfilled bars represent the incremental amount of carbon (0–24 h, $n = 3$; 24–72 h, $n = 2$; 72–120 h, $n = 1$) produced by respiration as a percentage of the total sugar and starch measured via the phenol-sulfuric acid method; filled bars represent 120-h totals ± SD. Error bars on 120-h totals represent $3\sigma^{24h}$, where σ^{24hr} is the standard deviation of the three replicate CO_2 concentrations measured at 24 h. In (b), bars represent the amount of carbon yielded from the ^{14}C extraction method, as a percentage of carbon expected based on total sugar and starch measured via the phenol-sulfuric acid method. In (c), over-yielding of the ^{14}C extraction method is dependent on initial sample mass, and primarily accounted for by the soluble nonstructural carbon extraction step, where blue circles represent additional samples of aspen twig, bark and wood. Note the broken axis in (b) and differing vertical scale in (b) and (c). See Figure S1 available as Supplementary data at *Tree Physiology* Online for full methodological workflow.

Extraction carbon yield

In comparison, carbon yield from the extraction-based ^{14}C method (which quantifies soluble nonstructural carbon and insoluble nonstructural carbon separately, so we summed these fractions) was universally higher than that expected based on summed sugar and starch phenol-sulfuric acid concentrations, ranging from 106 to 191% of expected carbon (Figure 2b). This 'over-yielding' appeared lowest in deep sapwood (106%) and highest in bark (191%), but additional replicate extractions show this variability is largely explained by sample mass used in the soluble carbon extraction step (Figure 2c). That is, when we included an extended range of dry tissue mass, we found observed yield in deep sapwood of near 100% was an artifact of saturation of the solution in sugars plus some combination of unknown solutes (Figure 2c). Put another way, as the ratio of sample mass to solute volume increases, a smaller proportion of sample solutes (unlikely to be all sugars) will be required to saturate the solution. Although the yield (of freeze-dried

solute mass) could be as high as 486% of expected soluble nonstructural carbon, the mean yield across all tissues and sample masses was 273 ± 101%, where 75% of the variation in yield of soluble nonstructural carbon can be explained by sample mass ($P < 0.001$, linear regression). Thus relative sugar carbon yield in all four tissues largely decreases with sample mass, and deep sapwood (106% carbon yield, Figure 2b) was merely the largest sample we analysed (Figure 2c, gray circle, lower right). High sample masses were necessary to achieve sufficiently large (target 1 mg C; Czimczik et al. 2014) insoluble carbon samples for a ^{14}C measurement (deep sapwood and heartwood contained low starch, Figure 1c). Water extracted material ('soluble nonstructural carbon') analyzed by HPAE-PAD clearly included some starch (3–5%), but sugars only constituted 22–42%, with a large majority (55–75%) being unidentified (Figure S3 available as Supplementary data at *Tree Physiology* Online).

$\Delta^{14}C$ agreement varies across tissues

Measures of $\Delta^{14}C$ (incubations, extracted soluble carbon, extracted insoluble carbon) were similar in sapwood, but strongly differed in bark and heartwood, where incubation $\Delta^{14}C$ was lower (younger, Figure 3). Respiration-weighted average $\Delta^{14}C$ from the incubation method was lowest in bark and highest in heartwood, increasing with radial depth. Thus, $\Delta^{14}C$ was 5 ± 2% (age = 2.4 ± 0.5 year) for bark, 6 ± 2% (2.6 ± 0.5 year) for shallow sapwood and 10 ± 2% (3.9 ± 0.5 year) for deep sapwood (Figure 3, filled triangles). Because so little carbon was respired by the heartwood (0.06 mg, Figure 2a), we were only able to obtain a single $\Delta^{14}C$ measurement for this tissue during the 24–72 h increment, with consequently low precision (22 ± 11%, 6.9 ± 2.4 years; Figure 3, open triangle). Mass-weighted average total bole $\Delta^{14}C$, using respired carbon mass from all tissues, gives mean incubation-based bole nonstructural carbon $\Delta^{14}C$ of 6.5% (8% ignoring bark), equivalent to an age of 2.9 years.

Extraction-based $\Delta^{14}C$ increased with depth into the bole xylem, where soluble and insoluble fractions tended to be similar, except for the bark. Thus, soluble fraction $\Delta^{14}C$ was 48 ± 2% (age = 12.4 ± 0.7 years) for bark, 2 ± 2% (1.9 ± 0.7 years) for shallow sapwood, 15 ± 2% (5.3 ± 0.5 years) for deep sapwood and 40 ± 2% (10.3 ± 0.5 years) for heartwood (Figure 3, filled circles). Extraction-based $\Delta^{14}C$ for the insoluble fraction was 18 ± 2% (5.9 ± 0.4 years) for bark, 1 ± 2% (1.5 ± 0.5 years) for shallow sapwood, 18 ± 2% (5.8 ± 0.4 years) for deep sapwood and 47 ± 2% (12.1 ± 0.7 years) for heartwood (Figure 3, filled squares). Overall mass-weighted $\Delta^{14}C$ of extracted nonstructural carbon (both soluble and insoluble carbon) was 47 ± 2% (11.8 ± 0.7 years) for bark, 2 ± 2% (1.8 ± 0.5 years) for shallow sapwood, 15 ± 2% (5.3 ± 0.5 years) for deep sapwood and 41 ± 2% (10.4 ± 0.5 years) for heartwood. Mass-weighted average total bole $\Delta^{14}C$ using the expected carbon mass (based on NSC concentrations) from all tissues gives a mean extraction-based bole nonstructural carbon $\Delta^{14}C$ of 35% (20% ignoring bark), equivalent to an age of 9.1 years.

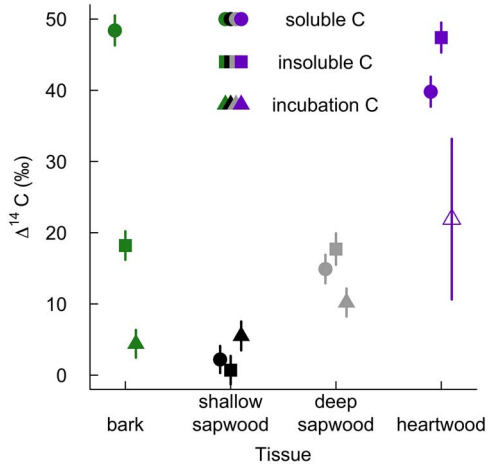

Figure 3. $\Delta^{14}C$ methods agree well in the sapwood, but agreement is poor in bark and heartwood, where incubation $\Delta^{14}C$ is much lower than those of either extracted soluble C or extracted insoluble C. Symbol denotes method/fraction—extraction soluble C (sugars): circles, extraction insoluble C (starch): squares, incubation C: triangles—for bark (green), shallow sapwood (black), deep sapwood (gray) and heartwood (purple). The single unfilled symbol denotes that $\Delta^{14}C$ was only available for a single time point (24–72 h) in the recent heartwood; other incubation $\Delta^{14}C$ were calculated from respired-mass (Figure 2) weighted averages of $\Delta^{14}C$ at the three incremental time points. Vertical lines denote the AMS error.

Time-series of incubation $\Delta^{14}C$

We assessed a time-series of $\Delta^{14}C$ of respired CO_2 at incremental time points along the 120-h incubations (24, 72 and 120 h). Despite extractions of oldest carbon in bark (soluble carbon, Figure 3), reverse-chronological mobilization was only weakly evident in deep sapwood (Figure 4). $\Delta^{14}C$ was essentially constant across incubation time in bark and shallow sapwood. Deep sapwood $\Delta^{14}C$ increased from 72 to 120 h by 8% (Figure 4). Respiration rates were also declining by 120 h (Figure 4b), where rates during the 72–120 h period were 26–46% lower compared with rates over the initial 24 h (Figure 4c). The full $\Delta^{14}C$ time-series was not available for heartwood as not enough carbon was produced.

Discussion

While we only measured a single tree, we suggest this may be a valuable approach to be considered by researchers interested in the cycling and age of nonstructural carbon in long-lived woody plants. Motivation for this study partially arose from observations of poor agreement between the mass obtained

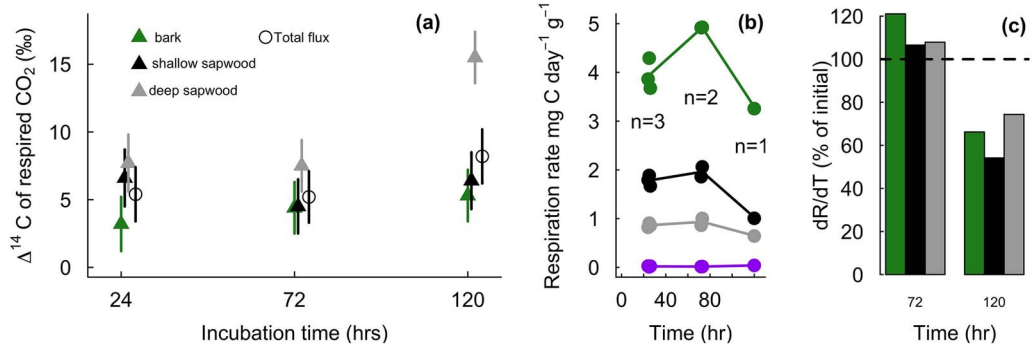

Figure 4. There is not clear evidence for reverse-chronological mobilization at the tissue level, suggesting $\Delta^{14}C$ from the incubation method is relatively robust to incubation time, and respiration rates were declining by 120 h. Colors denote tissue, for bark (green), shallow sapwood (black), deep sapwood (gray) and heartwood (purple). In (a), the mass-weighted incremental mean $\Delta^{14}C$ (entire increment core) is denoted by open circles. Symbols are jittered along the *x*-axis. Time-series $\Delta^{14}C$ data were not available for heartwood (not enough carbon produced). Vertical lines denote the AMS error. In (b), respiration rates are calculated as the 24-h production of C in incubations normalized to sample dry mass; note the declining sample size with time. In (c), respiration rates at 72 and 120 h are presented as % of the rate over the first 24 h; heartwood is omitted from (c) as respiration rates were extremely low.

from the extraction method and expectations based upon NSC concentrations in some tissues in *P. tremuloides*, where further attempts to purify extractions to isolate sugars (Rinne et al. 2012) also resulted in contamination of extracts. Essentially, the established extraction method did not appear to reliably isolate nonstructural carbon (Figure 2), where, for example, less than half of extracted soluble carbon is actually sugars (Figure S3 available as Supplementary data at *Tree Physiology* Online). The advantages and limitations of our alternative incubation method are noted in Table 2 as compared with the extraction method. In particular, whereas incubations capture less than 100% of measured sugars and starch carbon, not all extracted nonstructural carbon is likely available, metabolically relevant or (potentially) even nonstructural (Trumbore et al. 2015, Figure S3 available as Supplementary data at *Tree Physiology* Online). Although ages from both $\Delta^{14}C$ methods are consistent with previous work showing 'mixing in' of young nonstructural carbon into older tissues (Richardson et al. 2015), disagreement in $\Delta^{14}C$ values from incubations and extractions (Q1, Figure 3) suggests they sample non-identical carbon pools, particularly in bark and heartwood. Although we did not measure this, we hypothesize this is due to (i) tissue variation in extant living parenchyma, (ii) the role of carbohydrates in osmoregulation and, importantly (iii), incorporation of some carbon that is not reserve storage (potentially: hemicellulose, pectins, defensive compounds, Figure S3 available as Supplementary data at *Tree Physiology* Online). We briefly explore these explanations below. A potential criticism of this incubation method posits that respired carbon cannot be representative of the total nonstructural carbon pool if less than 100% of carbon is respired. However, time-series of incubations suggest $\Delta^{14}C$ from incubations is relatively robust to incomplete respiration of the total nonstructural carbon pool, at least in these tissues and species. This may be explained by the fact that sapwood was subsampled, and so all tissue in a given incubation was similarly aged. Incubating the entire sapwood, particularly from a tree with many sapwood rings, would likely give different results and is not recommended.

Extractions and incubations capture non-identical pools

A major result of this comparison is that the incubation method could be particularly valuable in older tree tissues. For example, heartwood or mixed-age tissues like bark contain dead parenchyma cells, where heartwood is essentially dead (Figure 2a and b, Spicer, 2005, 2016). Nonstructural carbon stored in dead cells would not be respired in incubations—but could be quantified in extractions. Then, nonstructural carbon in heartwood, while old according to extractions (higher $\Delta^{14}C$), is metabolically irrelevant (Furze et al. 2020). Sugar and starch concentrations and high extraction $\Delta^{14}C$ in the bark should be viewed with similar caution, particularly for the soluble carbon fraction, where $\Delta^{14}C$ is comparatively much lower for the insoluble fraction (Figure 3). Increasing frequency of dead parenchyma with sapwood depth (i.e., cell age) has also been shown in *Populus* hybrids (Nakaba et al. 2012) and particularly in *P. tremuloides* (Yang, 1993). Thus, we suggest that in our study, ~100% of parenchyma cells present in the outermost ring of the study tree were likely alive, whereas according to Yang (1993), this living cell proportion could drop as low ~60–70% at three-fourths of the sapwood depth. Thus, lower carbon yield (Figure 2a) and $\Delta^{14}C$ (Figure 3) of deep sapwood compared with extractions could reflect reduced proportion of living parenchyma in deeper rings.

Another potential advantage of incubations is comparatively more narrow characterization of the available nonstructural carbon pool, as osmolyte sugars are likely excluded. Complete (100%) respiration of nonstructural carbon is impossible, even in shallow sapwood, because cell turgor would be lost prior to 100% depletion as some proportion of sugars are involved

Table 2. Advantages and limitations of existing extraction method (Czimczik et al. 2014) and the proposed incubation method. For both methods, access to vacuum preparatory lines for CO_2 purification is assumed (purified CO_2 can be stored indefinitely and shipped to AMS facilities).

Method	Advantages	Limitations
Extractions	Potentially includes all water soluble and acid hydrolyzable nonstructural C	Poor specificity and over-yielding: non-reserve C, osmotic C, over-yield depends on extracted mass
	Sugar and starch fractions characterized separately	Sugar and starch separation appears unreliable
	Frozen tissue samples can be stored indefinitely	Vulnerable to fossil C (solvent) contamination
	Somewhat established	Insoluble C ('starch') samples can often be extremely small (<0.1 mg), reducing AMS utility
		Time intensive
		Some expensive equipment required (freeze drier)
		Does not capture lipid ^{14}C
Incubations	Only obtain available nonstructural C	Contribution of microbial decomposition to incubation CO_2 could be a concern in some tree species
	All respirable fractions are captured (likely including lipids)	Sugar and starch cannot be characterized independently
	Less time-intensive	Samples must be rapidly processed, including identifying tissue groupings, but this can be verified later
	Relatively inexpensive	Equipment (stabilizer cans, incubation chambers) and processing time can limit sample size on a given sampling day
	$\Delta^{14}C$ appears relatively independent of incubation time, though time may need adjustment for different species/tissues	Transport of glass jars is inconvenient, and chambers must be regularly assessed for leaks

in osmoregulation (Wang and Stutte 1992). In another study, nonstructural carbon consumption in aspen coarse roots forced to resprout in darkness (~22% in bark and ~42% in xylem) were strikingly similar to our estimates of incubation carbon production (22% in bark and 51% in deep sapwood; Figure 2a), but took place over a much longer time (up to 157 days; Wiley et al. 2019). This suggests incubations leverage the upregulation of respiration in response to stress from wounding induced by increment core collection (Uritani and Asahi, 1980) and may be a good approximation of available reserves. However, other compounds such as sugar alcohols (e.g., mannitol), organic acids (e.g., malic acid) and certain amino acids (e.g., proline) can be upregulated in response to drought and other stressors as osmoprotectants and to resist oxidative stress (Stoop et al. 1996, Guicherd et al. 1997, Tsamir-Rimon et al. 2021), and this sink (along with defensive compounds) might also compete with respiration during incubations to reduce yield compared with extractions. In contrast, extractions for ^{14}C cannot distinguish between 'osmotic' and 'storage' sugars at all; thus, each of these approaches may be more useful for different questions (Table 2).

Non-reserve C contribution to extraction $\Delta^{14}C$

Despite this, there appears to be an additional major limitation with extractions: they severely over-yield carbon (273 ± 101%, Figure 2c) much of which may not even be reserve/storage carbon (total sugars and starch represent only 25–46% of water extracts; Figure S3 available as Supplementary data at *Tree Physiology* Online). This over-yielding has also been shown in previous studies (Richter et al. 2009). Then, variability in the relative yield of the extraction method across tissues is explained by variation in initial dry sample mass, where carbon yields close to 100% are simply the result of saturation of the solution with various solutes during the soluble carbon ('sugars') extraction step (Figure 2c). In bulk aspen sapwood, non-sugar material constitutes an extremely variable percentage of hot water extracted solutions depending upon initial sample mass (48–370 mg, Figure S4 available as Supplementary data at *Tree Physiology* Online). Then, $\Delta^{14}C$ from extraction-based methods represents some combination of $\Delta^{14}C$ of nonstructural carbon (sugars, sugar alcohols, oligosaccharides, starch, amylose) plus other water soluble compounds (hemicelluloses, pectins, defensive compounds like phenolic glycosides or tannins, etc.). Organic acids and proteins may be metabolizable and thus serve as storage but many other compounds that are soluble in water may not. Hemicelluloses are often more abundant in wood than sugars Schädel et al. 2010), soluble in boiling water (Zhang et al. 2011) and unlikely to serve as reserves in non-reproductive tissues (Hoch, 2007). Defensive compounds could also be present in these extracts, where in *P. tremuloides* phenolic glycosides can occur at high concentrations in leaves (Kao et al. 2002). Finally, this species does store measurable concentrations of lipids (Grimberg et al. 2018). Lipids are not explicitly targeted by the ^{14}C extraction method (though some proportion of lipids may be extracted by hot water), and we are unaware of any method to do so, but lipids should be available for respiration in incubations. Separation of nonstructural carbon into soluble and insoluble fractions is ostensibly one of the advantages of the extraction method, but it also appears some starch is included in the soluble fraction (Figure S3 available as Supplementary data at *Tree Physiology* Online).

Evidence for reverse chronological mobilization

The absence of strong changes in $\Delta^{14}C$ across the time-series suggests $\Delta^{14}C$ from the incubation method is robust to incubation time (Figure 4a). Incubation time could be adjusted for different tissues or species, but at least in this species and tissue the assumption of 'last-in, first-out' dynamics (Lacointe et al. 1993, Muhr et al. 2018) in nonstructural carbon remobilization is not strongly supported. We only found increased $\Delta^{14}C$ with longer incubation time in deep sapwood, and only in the third time point, by 8%. This did not strongly change the $\Delta^{14}C$ of the total flux (Figure 4): the net effect of this additional ~ 30% of carbon on the total $\Delta^{14}C$ for deep sapwood is less than 3% (<1 year). We only measured a single tree in this study, but there are a number of reasons that this result may be somewhat general. For example, in a girdling study showing clear evidence of last-in, first out dynamics, or 'reverse chronological mobilization', the posited mechanism is spatial, rather than physiological (Muhr et al. 2018). That is, Muhr et al. (2018) suggest that reserves most proximal to the cambium, which are younger, are respired first. Given bark soluble carbon is the oldest measurement in this study (48 ± 2%, or ~10.4 year), we might expect a clear increase in $\Delta^{14}C$ with incubation time, as small additional amounts of the oldest carbon in this pool would strongly alter $\Delta^{14}C$. The absence of this effect suggests incubations are representative of the total nonstructural pool for a given tissue; but we might expect reverse chronological mobilization effects if tissues of varying ages were pooled in the same incubation (e.g., the whole sapwood; Muhr et al. 2018). Further, the declining respiration rates in the last 48-h period of the time-series (Figure 4b and c), coupled with very low CO_2 production in dead heartwood (Figure 2) suggests microbial contribution to CO_2 production is minimal or absent, and most of available nonstructural carbon had been respired. Tissue desiccation and mortality after 120 h might contribute to declining respiration rates, but again because shallow sapwood incubations yielded 85% of measured sugar and starch, we suggest this effect is small. We acknowledge longer incubation times may have led to stronger reverse chronological mobilization, but due to dead parenchyma, osmotica and dead tissue (e.g., heartwood, bark), we suggest it is unlikely this would greatly influence total $\Delta^{14}C$.

Thus, despite clear evidence for an apposition mechanism of starch granule formation in some species and organs, sometimes referred to as the 'onion model' (Badenhuizen and Dutton 1956, Pilling and Smith 2003), the relevance of this to carbon remobilization at larger scales is not apparent here. This is perhaps due to diurnal (Zeeman et al. 2007) or seasonal (Furze et al. 2019) starch interconversion to sugars, previously suggested to underlie very similar $\Delta^{14}C$ of sugar and starch pools in tree rings (Richardson et al. 2015). Also, the potential contribution of deeply stored starch in granules to overall nonstructural carbon mass is small here (starch concentrations are low, Figure 1), and starch was at least 90% exhausted in the sapwood following incubations. An alternative explanation is that reverse chronological mobilization emerges from probabilistic rather than physiological mechanisms (i.e., most nonstructural carbon is young, Herrera-Ramírez et al. 2020). Regardless, the influence of these dynamics seem to have a minor effect on age estimates from the incubation method described here, perhaps because the oldest C is more likely to be stored in dead parenchyma, and unlike starch, soluble sugars are more likely to be a well-mixed pool. Finally, we emphasize that in shallow sapwood, where nearly all parenchyma were likely living, more than 80% of measured sugars and starch were respired (Figure 2a). In short, despite that total tree nonstructural carbon is not a well-mixed pool (Herrera-Ramírez et al. 2020), this does not seem to matter in incubations of small numbers of sapwood tree rings or bark, with low influence on total $\Delta^{14}C$ (Figure 4a).

Conclusions

We demonstrated an incubation method that leverages cellular respiration of living tissue to estimate $\Delta^{14}C$ of nonstructural carbon. This method does have limitations (Table 2), such as the need to rapidly process collected samples, potential for leaking incubation chambers, inconvenience of transporting glass jars and potential for microbial contribution. This method has now only been assessed in *P. tremuloides*, yet the main advantage of incubations—capturing the nonstructural carbon that is actually metabolically available, including lipids—may make this a useful method for studying the cycling and metabolism of nonstructural carbon in other species. This method produced similar estimates to an extraction-based method in sapwood, but not bark and heartwood, where extraction-based $\Delta^{14}C$ should be viewed with caution. Sapwood $\Delta^{14}C$ differed by at most ~ 5% (or a difference of 1.4 years) between methods. In heartwood and bark, method disagreement in nonstructural carbon mass and $\Delta^{14}C$ is potentially due to the presence of dead parenchyma cells containing extractable nonstructural carbon, as well as universal over-yielding and poor specificity of the extraction method (Figure 2). That is, the ^{14}C extraction method is including carbon in excess of the sugar and starch pools (Figure S3 available as Supplementary data at *Tree Physiology* Online). To put this in perspective, mean bole nonstructural carbon $\Delta^{14}C$ was 29% higher with the extraction method—this is equivalent to a 6-year (or threefold) difference in age between methods. We highlight similar concerns might be considered by those making sugar and starch concentration measurements in diverse tissues, where sampling coarse branches and roots with heartwood tissue may result in overestimates of available nonstructural carbon. Finally, this work validates an alternative approach to study the role and availability of nonstructural carbon in different tissues, thus potentially permitting more routine incorporation of

$\Delta^{14}C$ into eco-physiological studies of tree response to stress and disturbance.

Supplementary data

Supplementary data for this article are available at *Tree Physiology* Online.

Acknowledgments

We thank Mark Nabel for his help in identifying a study tree, Michael Chizhov for assistance harvesting, and George Koch for early method feedback.

Funding

This work was funded by NSF-IOS-RAPID (#1936205 and #2053337). Early work on the method was funded by a NSF-DEB Doctoral Dissertation Improvement Grant (#DEB-1702017).

Authors' contributions

D.M.P.P. developed the incubation method with input from K.O., C.E. and X.X. D.M.P.P. conceived the study with guidance from M.S.C. and A.D.R. D.M.P.P. and J.L. collected the data. D.M.P.P. analysed the data and wrote the first draft of the manuscript. All authors significantly contributed to revisions.

Data availability statement

The data that support the findings of this study are available in the supplementary material of this article.

Conflict of interest

None declared.

References

Badenhuizen NP, Dutton RW (1956) Growth of ^{14}C-labelled starch granules in potato tubers as revealed by autoradiographs. Protoplasma 47:156–163.

Boutton TW, Wong WW, Hachey DL, Lee LS, Cabrera MP, Klein PD (1983) Comparison of quartz and pyrex tubes for combustion of organic samples for stable carbon isotope analysis. Anal Chem 55:1832–1833.

Cain WF, Suess HE (1976) Carbon 14 in tree rings. J Geophys Res 81:3688–3694.

Carbone MS, Trumbore SE (2007) Contribution of new photosynthetic assimilates to respiration by perennial grasses and shrubs: residence times and allocation patterns. New Phytol 176:124–135.

Carbone MS, Czimczik CI, McDuffee KE, Trumbore SE (2007) Allocation and residence time of photosynthetic products in a boreal forest using a low-level ^{14}C pulse-chase labeling technique. Glob Change Biol 13:466–477.

Carbone MS, Czimczik CI, Keenan TF, Murakami PF, Pederson N, Schaberg PG, Xu X, Richardson AD (2013) Age, allocation and availability of nonstructural carbon in mature red maple trees. New Phytol 200:1145–1155.

Czimczik CI, Trumbore SE, Xu XM, Carbone MS (2014) Extraction of nonstructural carbon and cellulose from wood for radiocarbon analysis. Bio Protoc 4:e1169.

Dietze MC, Sala A, Carbone MS, Czimczik CI, Mantooth JA, Richardson AD, Vargas R (2014) Nonstructural carbon in woody plants. Annu Rev Plant Biol 65:667–687.

Epron D, Bahn M, Derrien D et al., others (2012) Pulse-labelling trees to study carbon allocation dynamics: a review of methods, current knowledge and future prospects. Tree Physiol 32:776–798.

Furze ME, Huggett BA, Aubrecht DM, Stolz CD, Carbone MS, Richardson AD (2019) Whole-tree nonstructural carbohydrate storage and seasonal dynamics in five temperate species. New Phytol 221:1466–1477.

Furze ME, Huggett BA, Chamberlain CJ et al. (2020) Seasonal fluctuation of nonstructural carbohydrates reveals the metabolic availability of stemwood reserves in temperate trees with contrasting wood anatomy. Tree Physiol 40:1355–1365.

Gartner BL, Baker DC, Spicer R (2000) Distribution and vitality of xylem rays in relation to tree leaf area in Douglas-fir. IAWA J 21:389–401.

Grimberg Å, Lager I, Street NR, Robinson KM, Marttila S, Mähler N, Ingvarsson PK, Bhalerao RP (2018) Storage lipid accumulation is controlled by photoperiodic signal acting via regulators of growth cessation and dormancy in hybrid aspen. New Phytol 219: 619–630.

Guicherd P, Peltier JP, Gout E, Bligny R, Marigo G (1997) Osmotic adjustment in Fraxinus excelsior L.: malate and mannitol accumulation in leaves under drought conditions. Trees 11:155–161.

Herrera-Ramírez D, Muhr J, Hartmann H, Römermann C, Trumbore S, Sierra CA (2020) Probability distributions of nonstructural carbon ages and transit times provide insights into carbon allocation dynamics of mature trees. New Phytol 226:1299–1311.

Hilman B, Muhr J, Helm J, Kuhlmann I, Schulze E-D, Trumbore S (2021) The size and the age of the metabolically active carbon in tree roots. Plant Cell Environ 44:2522–2535.

Hoch G (2007) Cell wall hemicelluloses as mobile carbon stores in non-reproductive plant tissues. Funct Ecol 21:823–834.

Hoch G, Richter A, Körner C (2003) Non-structural carbon compounds in temperate forest trees. Plant Cell Environ 26:1067–1081.

Hua Q, Barbetti M (2004) Review of tropospheric bomb ^{14}C data for carbon cycle modeling and age calibration purposes. Radiocarbon 46:1273–1298.

Hua Q, Turnbull JC, Santos GM et al. (2021) Atmospheric radiocarbon for the period 1950–2019. Radiocarbon 64:723–745.

Kao Y-Y, Harding SA, Tsai C-J (2002) Differential expression of two distinct phenylalanine ammonia-lyase genes in condensed tannin-accumulating and lignifying cells of quaking aspen. Plant Physiol 130:796–807.

Keeling CD (1979) The Suess effect: ^{13}Carbon-^{14}Carbon interrelations. Environ Int 2:229–300.

Kozlowski TT (1992) Carbohydrate sources and sinks in woody plants. Bot Rev 58:107–222.

Lacointe A, Kajji A, Daudet F-A, Archer P, Frossard J-S, Saint-Joanis B, Vandame M (1993) Mobilization of carbon reserves in young walnut trees. Acta Bot Gallica 140:435–441.

Landhäusser SM, Chow PS, Dickman LT et al. (2018) Standardized protocols and procedures can precisely and accurately quantify nonstructural carbohydrates. Tree Physiol 38:1764–1778.

Lehmann MM, Gamarra B, Kahmen A, Siegwolf RT, Saurer M (2017) Oxygen isotope fractionations across individual leaf carbohydrates in grass and tree species. Plant Cell Environ 40:1658–1670.

Levin I, Kromer B (2004) The tropospheric $^{14}CO_2$ level in mid latitudes of the northern hemisphere (1959-2003). Radiocarbon 46:1261–1271.

Lowe DC (1984) Preparation of graphite targets for radiocarbon dating by tandem accelarator mass spectrometer (TAMS). Int J Appl Radiat Isot 35:349–352.

Matamala R, Gonzalez-Meler MA, Jastrow JD, Norby RJ, Schlesinger WH (2003) Impacts of fine root turnover on forest NPP and soil C sequestration potential. Science 302:1385–1387.

Muhr J, Messier C, Delagrange S, Trumbore S, Xu X, Hartmann H (2016) How fresh is maple syrup? Sugar maple trees mobilize carbon stored several years previously during early springtime sap-ascent. New Phytol 209:1410–1416.

Muhr J, Trumbore S, Higuchi N, Kunert N (2018) Living on borrowed time–Amazonian trees use decade-old storage carbon to survive for months after complete stem girdling. New Phytol 220: 111–120.

Nakaba S, Begum S, Yamagishi Y, Jin H-O, Kubo T, Funada R (2012) Differences in the timing of cell death, differentiation and function among three different types of ray parenchyma cells in the hardwood *Populus sieboldii* × *P. grandidentata*. Trees 26:743–750.

Pearson LC, Lawrence DB (1958) Photosynthesis in aspen bark. Am J Bot 45:383–387.

Peltier DM, Barber JJ, Ogle K (2018) Quantifying antecedent climatic drivers of tree growth in the Southwestern US. J Ecol 106:613–624.

Pilling E, Smith AM (2003) Growth ring formation in the starch granules of potato tubers. Plant Physiol 132:365–371.

Plain C, Gerant D, Maillard P, Dannoura M, Dong Y, Zeller B, Priault P, Parent F, Epron D (2009) Tracing of recently assimilated carbon in respiration at high temporal resolution in the field with a tuneable diode laser absorption spectrometer after in situ $^{13}CO_2$ pulse labelling of 20-year-old beech trees. Tree Physiol 29:1433–1445.

Quentin AG, Pinkard EA, Ryan MG et al. (2015) Non-structural carbohydrates in woody plants compared among laboratories. Tree Physiol 35:1146–1165.

Raessler M, Wissuwa B, Breul A, Unger W, Grimm T (2010) Chromatographic analysis of major non-structural carbohydrates in several wood species–an analytical approach for higher accuracy of data. Anal Methods 2:532–538.

Reimer PJ, Brown TA, Reimer RW (2004) Discussion: reporting and calibration of post-bomb ^{14}C data. Radiocarbon 46:1299–1304.

Richardson AD, Carbone MS, Huggett BA, Furze ME, Czimczik CI, Walker JC, Xu X, Schaberg PG, Murakami P (2015) Distribution and mixing of old and new nonstructural carbon in two temperate trees. New Phytol 206:590–597.

Richardson AD, Carbone MS, Keenan TF, Czimczik CI, Hollinger DY, Murakami P, Schaberg PG, Xu X (2013) Seasonal dynamics and age of stemwood nonstructural carbohydrates in temperate forest trees. New Phytol 197:850–861.

Richter A, Wanek W, Werner RA et al. (2009) Preparation of starch and soluble sugars of plant material for the analysis of carbon isotope composition: a comparison of methods. Rapid Commun Mass Spectrom 23:2476–2488.

Rinne KT, Saurer M, Streit K, Siegwolf RT (2012) Evaluation of a liquid chromatography method for compound-specific $\delta^{13}C$ analysis of plant carbohydrates in alkaline media. Rapid Commun Mass Spectrom 26:2173–2185.

Rocha AV, Goulden ML, Dunn AL, Wofsy SC (2006) On linking interannual tree ring variability with observations of whole-forest CO_2 flux. Glob Change Biol 12:1378–1389.

Schädel C, Blöchl A, Richter A, Hoch G (2010) Quantification and monosaccharide composition of hemicelluloses from different plant functional types. Plant Physiol Biochem 48:1–8.

Schuur EA, Trumbore SE (2006) Partitioning sources of soil respiration in boreal black spruce forest using radiocarbon. Glob Change Biol 12:165–176.

Schuur EA, Druffel ER, Trumbore SE (2016) Radiocarbon and climate change. Springer, Switzerland.

Spicer R (2005) Senescence in secondary xylem: heartwood formation as an active developmental program. In: Holbrook NM, Zwieniecki MA (eds), Vascular Transport in Plants. Academic Press 457–475.

Spicer R (2016) Variation in angiosperm wood structure and its physiological and evolutionary significance. In: Groover A, Cronk Q (eds), Comparative and evolutionary genomics of angiosperm trees. Springer, Switzerland, pp 19–60.

Stoop JM, Williamson JD, Pharr DM (1996) Mannitol metabolism in plants: a method for coping with stress. Trends Plant Sci 1:139–144.

Stuiver M, Polach HA (1977) Discussion reporting of ^{14}C data. Radiocarbon 19:355–363.

Synal H-A, Stocker M, Suter M (2007) MICADAS: a new compact radiocarbon AMS system. Nucl Instrum Methods Phys Res Sect B Beam Interact Mater At 259:7–13.

Trumbore S, Czimczik CI, Sierra CA, Muhr J, Xu X (2015) Nonstructural carbon dynamics and allocation relate to growth rate and leaf habit in California oaks. Tree Physiol 35:1206–1222.

Tsamir-Rimon M, Ben-Dor S, Feldmesser E, Oppenhimer-Shaanan Y, David-Schwartz R, Samach A, Klein T (2021) Rapid starch degradation in the wood of olive trees under heat and drought is permitted by three stress-specific beta amylases. New Phytol 229:1398–1414.

Uritani I, Asahi T (1980) Respiration and related metabolic activity in wounded and infected tissues. In: Metabolism and Respiration. Elsevier, pp 463–485.

Vargas R, Trumbore SE, Allen MF (2009) Evidence of old carbon used to grow new fine roots in a tropical forest. New Phytol 182:710–718.

Vogel JS, Southon JR, Nelson DE, Brown TA (1984) Performance of catalytically condensed carbon for use in accelerator mass spectrometry. Nucl Instrum Methods Phys Res B 5:289–293.

Wang Z, Stutte GW (1992) The role of carbohydrates in active osmotic adjustment in apple under water stress. J Am Soc Hort Sci 117:816–823.

Wiley E, King CM, Landhäusser SM (2019) Identifying the relevant carbohydrate storage pools available for remobilization in aspen roots. Tree Physiol 39:1109–1120.

Yang KC (1993) Survival rate and nuclear irregularity index of sapwood ray parenchyma cells in four tree species. Can J For Res 23:673–679.

Zeeman SC, Smith SM, Smith AM (2007) The diurnal metabolism of leaf starch. Biochem J 401:13–28.

Zhang Y, Hosseinaei O, Wang S, Zhou Z (2011) Influence of hemicellulose extraction on water uptake behavior of wood strands. Wood Fiber Sci 43:244–250.